Hindawi
Journal of Sensors
Volume 2019, Article ID 2374246, 11 pages
https://doi.org/10.1155/2019/2374246

Research Article

Characteristic of Magnetic Fluctuation of Underground Passing Pig Labeled with Magnets

Wei Xu,[1] Zhiyong Guo,[1] Pan Wu,[1] and Wenhui Chen[2]

[1]*School of Mechatronic Engineering, Southwest Petroleum University, Chengdu 610500, China*
[2]*China Petroleum Engineering & Construction Corp Beijing Company, Beijing 100085, China*

Correspondence should be addressed to Zhiyong Guo; zhyguo@swpu.edu.cn

Received 11 October 2018; Revised 20 December 2018; Accepted 6 January 2019; Published 17 February 2019

Academic Editor: Carmine Granata

During the pigging process, a pig labeled with magnets can be effectively detected by monitoring the magnetic fluctuation (MF) introduced when the pig passes by. In order to analyze the influence of various factors on the MF, the principle for magnetic fluctuation detection (MFD) is described, and a detection model is established here. The influence of model parameters, such as pipeline geometries, geomagnetic characteristics, as well as permeability of pipeline, on the magnetic anomaly distribution along the measured line is analyzed. The study reveals that with the increase in pipeline parameters (thickness, permeability, and outer diameter), the MF detected decreases. The pipeline length will have little influence on the MF. With an increased number of magnets, the MF increases while remaining almost unchanged at two ends of the measuring line. Attention should be paid to the installation of magnets to ensure the consistency of the magnetic moments. With the increase in geomagnetic intensity and declination, the MF will be almost unaffected, while the change of geomagnetic inclination will introduce an obvious change to the MF. In field application, measuring points can be set along and above the pipeline with a certain interval. From the magnetic anomaly measured, it can be determined whether the pig has passed by the point or not.

1. Introduction

After a long-time operation, large-diameter oil and gas pipelines need to be cleaned regularly due to the remaining dirt [1, 2]. In the cleaning process, it is easy for the pig to get blocked, leading to serious consequences [2]. Therefore, it was of great importance to divide the pipeline into segments and monitor the real-time condition per segment. In this way, the excavation and rescue of the pig can be performed timely when it is trapped [3]. At present, the technologies for tracking and positioning of the pig mainly consist of a radioactive isotope method, mileage wheel method, acoustic method, pressure pulse method, and magnetic method. Qiu et al. analyzed the advantages and disadvantages of the abovementioned traditional technologies. They pointed out that the electromagnetic pulse method and stress method were the best and most stable technologies of the five. They also put forward a kind of online tracking method based on the fiber optic vibration principle which could monitor the position of the pig [3]. Because fiber optical vibration detection has high sensitivity, it is easy to be influenced by the vibration sources such as cars passing by. In order to achieve the monitoring, it is necessary to lay a fiber optical cable along the pipeline. Since the laying of the cable constitutes a huge workload for the project, this approach is therefore deemed to be practical only for some particular cases [3].

Owing to the simplicity of the signal source and detection unit, magnetostatic detection has its unique advantages compared with other methods [4, 5]. The magnetic anomaly detection (MAD) method is one of the methods for pig detection [4, 6, 7]. Magnetic anomaly detection methods began to emerge and develop in the 1990s [8]. Currently, MAD is mainly based on the analysis of magnetic anomaly distribution within the measuring surface or measuring line [5, 6, 9, 10], so as to identify and position a magnetic source such as the unexploded ordnance (UXO) [11], the underground pipeline [6, 12–14], and the underground iron wastes [15, 16]. The parameters of the magnetic dipole are retrieved according to the magnetic properties of the magnetic dipole

[17]. The application of MAD is unusual to see nowadays. Related researches mainly include Li et al. who placed a miniature diagnostic and treatment device in the human gut and calculated the position of the magnetic device by monitoring the magnetic field outside the human body [18]. Based on the detection of changes of the magnetic field induced by the magnet in the capsule endoscope, Hu et al. proposed a new positioning algorithm to track the position of the endoscope [19, 20]. Baldoni and Yellen developed a magnetic tracking system to detect the operation and performance of the mechanical heart valve [21]. Due to the rapid development of various magnetic sensors [22, 23], the research and application of magnetic anomaly detection in the above fields can be completed by experiments, but the experiments have some limitations, and only one case can be analyzed separately. For the positioning of the magnetic source identification pig, there are many factors affecting the positioning accuracy. If the work is done by experiment alone, the workload is very large. Therefore, the method of numerical simulation can be used to analyze the factors separately. To sum up, the MF has already been put into use of tracking and positioning of materials [5, 18, 19]. But the application in tracking of magnet-labeled pig in the pipeline is relatively rare to see. And the influences of pipeline geometries, pipeline permeability, and permanent magnet setup on magnetic anomaly fluctuations still remain to be further studied [6].

In order to verify the feasibility and effectiveness of the method which calculates the position of the pig by detecting the MF, a mathematical model is established based on a magnet-labeled pig [6, 24]. The influencing factors of MF are fully analyzed. At the same time, related experiments are designed to prove the correctness of the simulation results. All the studies in this paper will play a theoretically fundamental role in guiding the design of the prototype of the detection device proposed and at the same time support the analytical study of the measured datum [6].

2. Methods

2.1. Model Parameters. As shown in Figure 1, in the Cartesian coordinate system, the origin of the coordinate is at the center of the geometry. The axis of the pipeline is the y-axis. The pig which is mounted with magnets moves from left to right in the pipeline. Let us assume that the space for the finite element method is confined within the cuboid area, whose length is L_s, width is D_s, and height is H_s [6, 13]. As shown in Figures 2 and 3, the outer diameter of the pipeline is D_d, and the thickness is δ. The distance between the measuring surface and the pipeline axis is h [6].

2.2. Theoretical Derivation. The geomagnetic field H_b is a vector characterized by both magnitude and direction. The nature of the geomagnetic field is that every ferromagnetic material within it will be magnetized to be magnetic. Within a small geographical area and a short period of time, the geomagnetic field could be regarded as constant [25, 26]. For such a static magnetic field with no electric current as the geomagnetic field, the following equation shall apply:

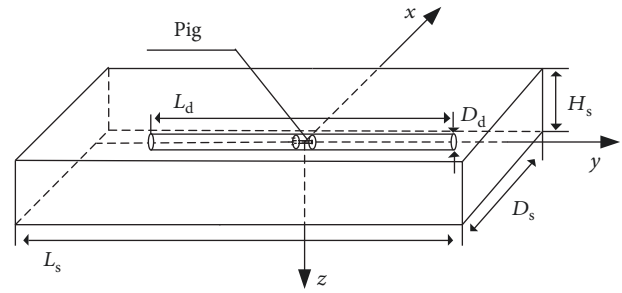

Figure 1: Geometric model of the magnetic source.

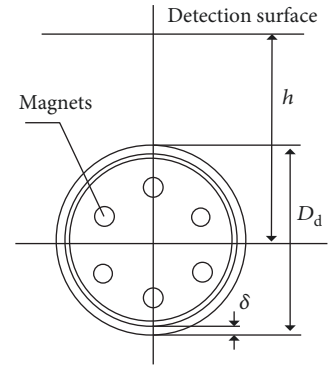

Figure 2: Vertical profile of the pig with magnets in the pipe.

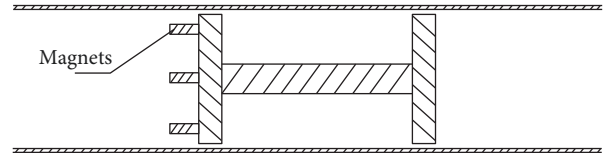

Figure 3: Horizontal profile of the pig with magnets in the pipe.

$$\nabla \times H = 0, \qquad \nabla \cdot B = 0. \tag{1}$$

The magnet is characterized by a wide hysteresis loop, high coercivity, and high remanence. Once magnetized, it will become magnetic with constant magnetism [20]. The magnets, which are mounted on the pig, will magnetize the surrounding magnetic material and thus introduce some changes to the magnetic field of the area [6, 16]. In the numerical simulation, the residual flux density is used to describe the properties of the magnet, which is given by

$$B = u_0 u_r H + B_r, \tag{2}$$

where B_r is the intensity of remanence.

For the boundary conditions in finite element analysis, the external flux density is used in the paper. The boundaries

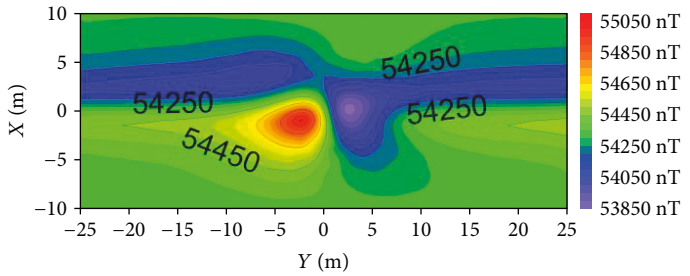

Figure 4: Detection distribution of the magnetic field of a pig with magnets in the pipeline.

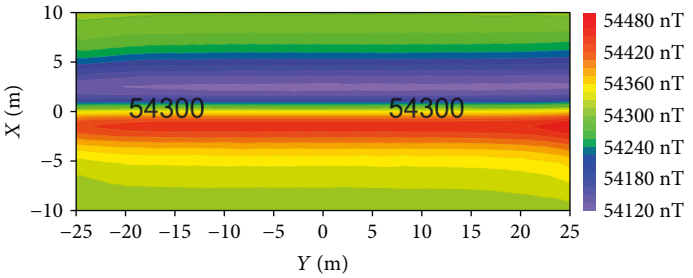

Figure 5: Detection distribution of the magnetic field of a pig without any magnet.

applied are the six surfaces of the cuboid [24]. The boundary condition is given by

$$n \cdot B_1 = n \cdot B_2. \tag{3}$$

For the magnetization process of the pipeline, Equation 2 still applies and here B_r is assumed to be 0.

3. Model Analysis

3.1. Model Characterization. The international geomagnetic field in Langfang, Hebei Province, China, in 2017 is specified as the excitation field in model establishment. The total magnetic intensity of the area is 54339.8 nT, magnetic declination is -6.807°, and magnetic inclination is 58.540° [25, 26]. Let us assume that the measuring surface is always above the ground, and the section 3.5 m away from the pipeline is specified as the measuring surface. The basic parameters of the cuboid are assumed to be as follows: the length is 100 m, the width is 20 m, and the height is 10 m. The length of the pipeline is 70 m, the outer diameter is 0.5 m, and the wall thickness is 10 mm. The length of the pig is 1 m. The outer diameter of the end face of the pig is 0.45 m. Six identical magnets are evenly and symmetrically distributed on one end of the pig. The default permeability of the pipeline is 900. The pipeline is placed along the y-axis and located at the center of the cuboid. The pig is placed at the middle of the pipeline at the beginning.

In order to verify the effectiveness of the magnetic source in causing MF, two pigs are employed in the simulation. One is equipped with a magnetic source, while the other is not [16, 24]. The magnetic source is composed of six cylindrical magnets, each with a residual flux density of 1.2 T and a

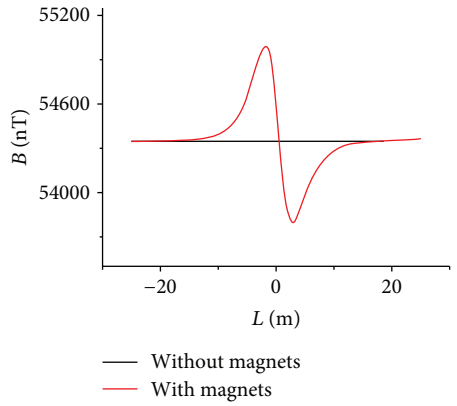

Figure 6: The influence of magnets on the magnetic anomaly on the measuring line.

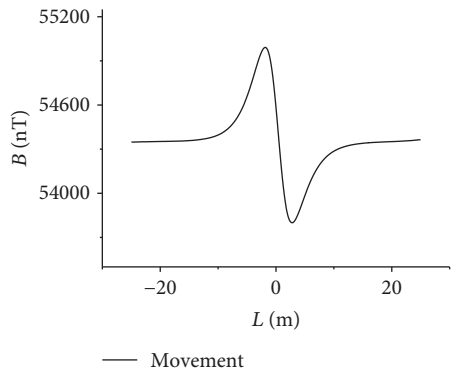

Figure 7: The influence of the movement of magnets on the MF at the measuring point.

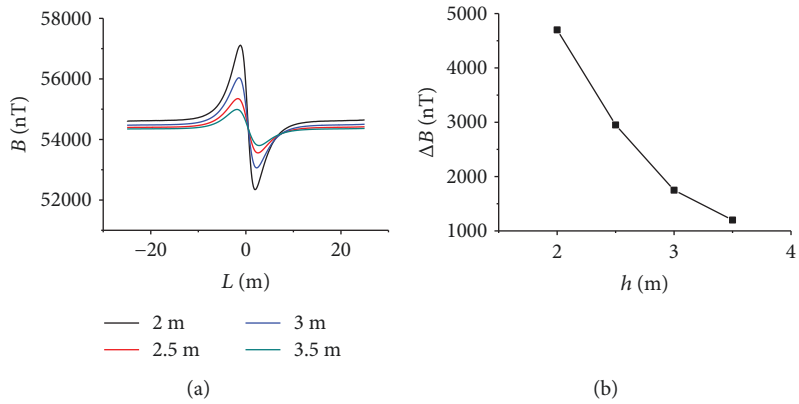

Figure 8: The influence of pipeline buried depth on MF. (a) Four MF curves; (b) the variation trend of MF.

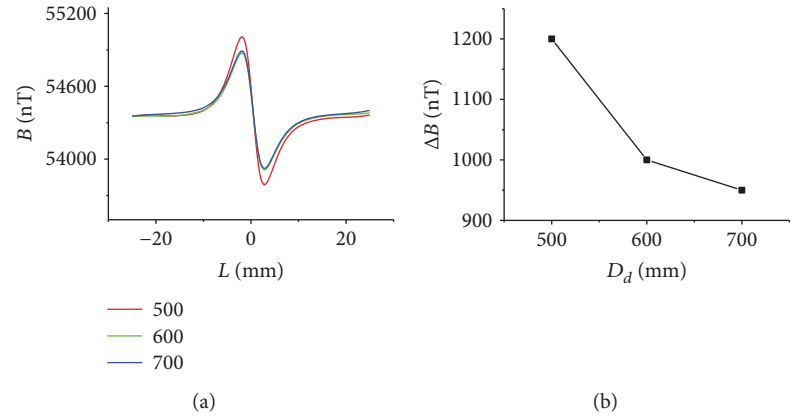

Figure 9: The influence of pipeline outer diameter on MF. (a) Three MF curves; (b) the variation trend of MF.

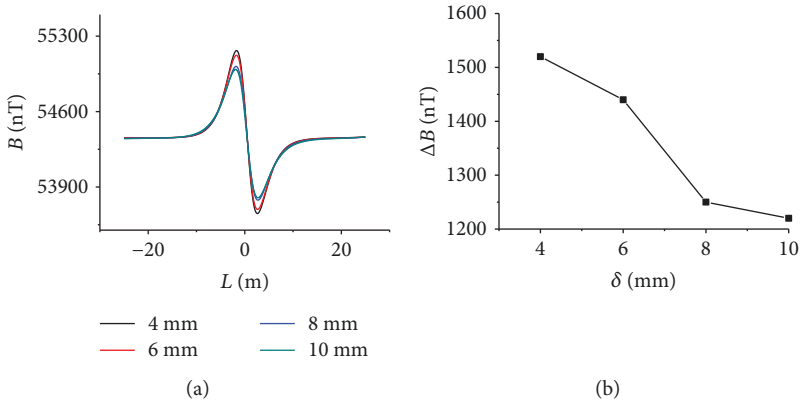

Figure 10: The influence of the pipeline wall thickness on MF. (a) Four MF curves; (b) the variation trend of MF.

magnetic moment pointing to the forward direction of the y-axis, the diameter of the magnet is 50 mm, and the length is 60 mm. Figure 4 gives the distribution of the measured magnetic field where the pig is equipped with magnets. Figure 5 corresponds to the pig without any magnet.

Comparing Figures 4 and 5, it can be seen that with the same model parameters, the existence of magnets will have a very obvious effect on the magnetic distribution on the measuring surface. As Figure 4 shows, the magnets cause disturbances of the magnetic field above the pig. The smooth distribution of the magnetic field becomes curved, and the maximum intensity increases. Based on this phenomenon observed, the position of the pig could be roughly determined [16, 24]. In order to further analyze the influence of the magnetic source, a three-dimensional transversal line which is 3.5 m above and stretches along the pipeline axis is specified as the measuring line. The distribution of the magnetic field along this line is shown in Figure 6. It can be seen from

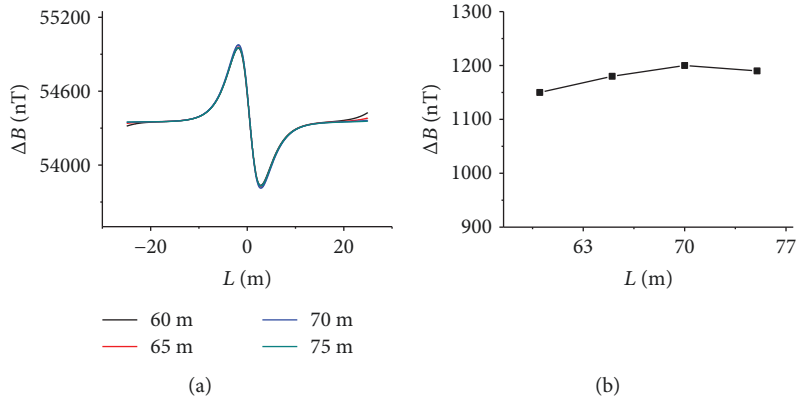

Figure 11: The influence of pipeline length on magnetic anomaly. (a) Four MF curves; (b) the variation trend of MF.

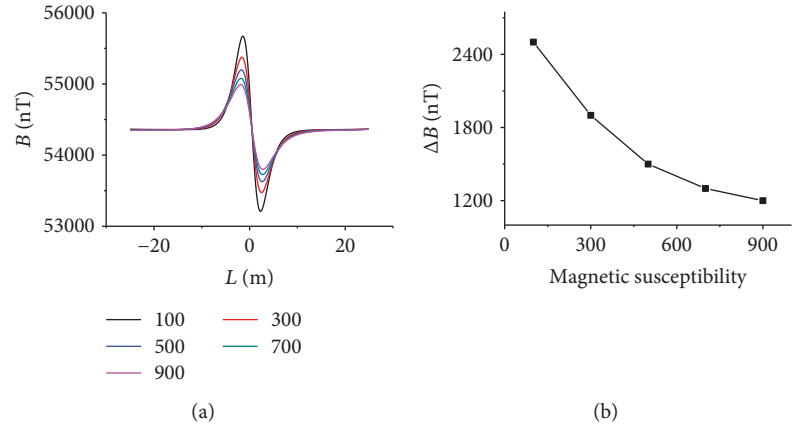

Figure 12: The influence of permeability of the pipeline on MF. (a) Five MF curves; (b) the variation trend of MF.

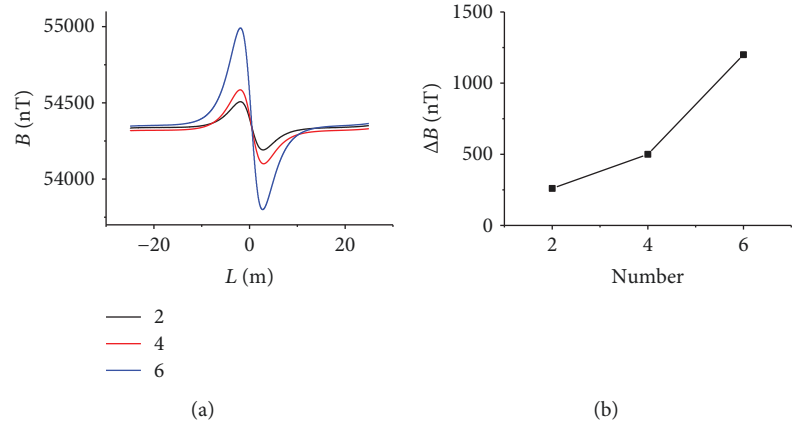

Figure 13: The influence of the numbers of magnets on the MF. (a) Three MF curves; (b) the variation trend of MF.

the figure that the magnets mounted on the pig induce obvious MF along the measuring line. The magnetic field stays steady at first, then it rises to the peak and drops to the valley and finally becomes steady again [6]. The maximum magnetic fluctuation caused by permanent magnets is about 1200 nT. The results measured by the measuring line are almost consistent with those by the measuring surface.

When the pig is in motion, in order to study the influence of the pig on the MF at the measuring point, the measuring point is specified to be placed at (0,0,3.5) with the range of measuring line being $x = -25$ m to $x = 25$ m. Assume that the pig with permanent magnets is moving at a constant speed. The influence of the pig's position on the magnetic anomaly fluctuation at the measuring point is analyzed. As

shown in Figure 7, since at both ends of the curve it is far away from the measuring point, the magnets impose a weak influence. So the measuring step is chosen to be relatively larger. But from $x = -15$ m to $x = 15$ m, the step is set to be 0.2 m. In this way, the simulation results are closer to the actual measuring results. It can be seen from the figure that the MF at the measuring point also goes through a steady-rise-drop-steady process [6]. When the pig is far away from the measuring point, the MF at the measuring point is relatively stable. When the pig approaches the measuring point, the magnetic anomaly at the measuring point fluctuates violently. The maximum fluctuation is about 1200 nT. The MF becomes steady again when the pig departs from the measuring point. Because of the basic consistency between the magnetic anomaly of the measuring line and the measuring point, in the latter study, the magnetic anomaly of the measuring line can be used to replace the magnetic anomaly at the measuring point.

3.2. Analysis of Influencing Factors. In order to study the influencing factors of the MF, the model parameters in Section 3.1 will be studied one by one. When analyzing the influencing factors, there will be only one variable in each analysis and the other parameters shall remain constant.

3.2.1. Pipeline Buried Depth. As a normal engineering practice, the pipeline buried depth will be determined considering many factors including the complex geographical structures, and it will be subject to many restrictions such as the underground water, underground cavity, hard rocks, and existing pipelines [5, 11, 12, 14]. In order to simulate different buried depths of the pipeline, different distances between the pipeline and the measuring line are used in the simulation. By keeping the other model parameters unchanged, the distance h varies from 2 m to 3.5 m, with an interval of 0.5 m. The measuring results of magnetic anomaly along the measuring line are shown in Figure 8.

It can be seen from Figure 8 that, with the increase in the distance between the measuring line and the pipeline, the MF decreases from 4700 nT to 1200 nT correspondingly.

3.2.2. Pipeline Geometries. The pipeline geometric parameters include pipeline outer diameter, wall thickness, and pipeline length. The different pipelines with different geometries will be needed for specific applications in engineering [6]. In order to study the influence of pipeline geometries on MAD, each geometric parameter will be studied separately. For each study, the parameter to be studied will be specified as variable and the others constant. In terms of analysis of the pipeline outer diameter, Figure 9 gives the simulation results where the diameter varies from 500 mm to 700 mm with an interval of 100 mm.

It can be seen from Figure 9 above that with the increase in the pipeline outer diameter, the magnetic anomaly at both ends of the measuring line almost remains unchanged. But the magnetic anomaly above the permanent magnets decrease correspondingly, ranging from 1200 nT to 950 nT. The reason is that when the pipeline diameter increases, the shielding effect of the pipeline on the magnetic field is

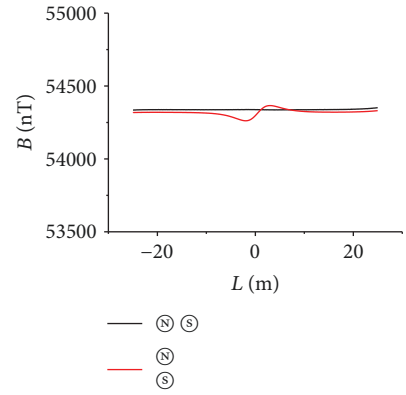

Figure 14: The influence of polarity of permanent magnets on the magnetic anomaly.

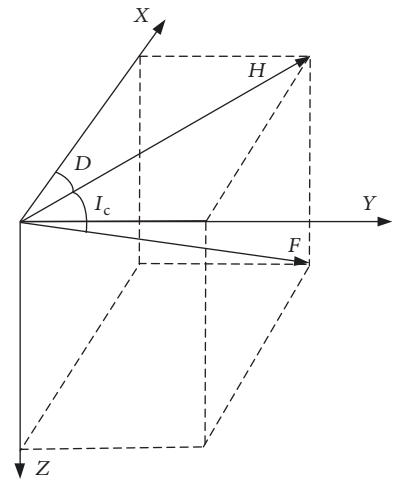

Figure 15: The distribution of the geomagnetic field.

enhanced. Therefore, the magnetic anomaly induced by the permanent magnets will be detected more difficultly and the magnitude will be smaller.

In order to analyze the influence of the wall thickness on the MF, the wall thickness is specified to be from 4 mm to 10 mm, with an interval of 2 mm. The simulation results are shown in Figure 10.

The simulation results indicate that the change in pipeline thickness will cause a nonlinear change of MF. But with the increase in the wall thickness, the MF decreases gradually. The main reason is that an increased wall thickness will result in more magnetic shielding. In the simulation, the MF ranges from 1500 nT to 1200 nT.

Pipeline length can be from a few meters to thousands of meters, and even thousands of kilometers. But in the simulation study, it is very difficult to simulate thousands of kilometers of pipeline, and it is of little significance to do so [6, 24]. On the other hand, a short pipeline of several meters long is also hard to simulate due to the leakage of the magnetic flux at both ends of the pipeline [6]. Against this, the pipeline length is specified to be from 60 m and 75 m with an interval of 5 m in the following study. And the

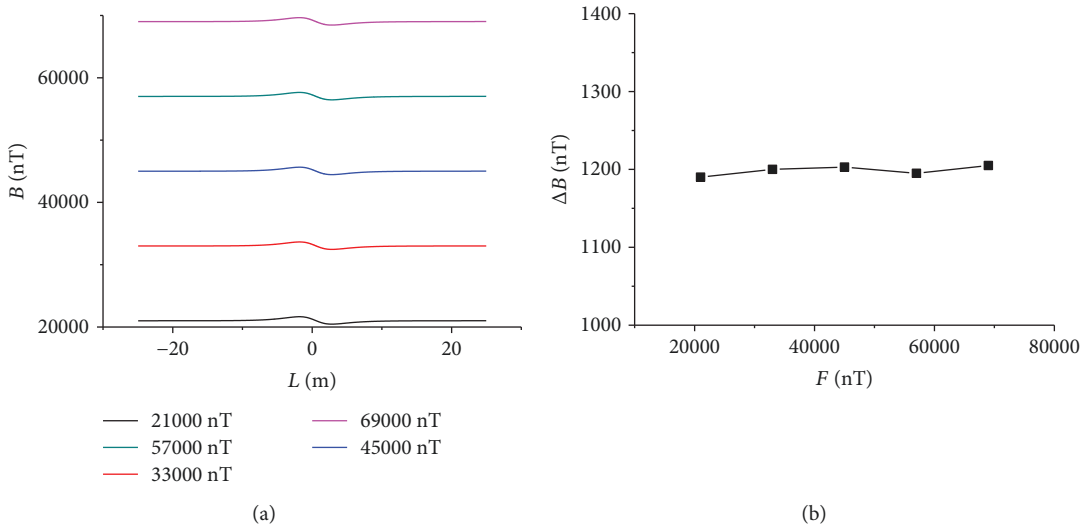

Figure 16: The influence of geomagnetic intensity on magnetic anomaly. (a) Five MF curves; (b) the variation trend of MF.

simulation results of the influence of pipeline length on magnetic anomaly are obtained and shown in Figure 11.

The simulation results indicate that for different lengths of pipeline, the magnetic anomalies measured almost remain the same which slightly vary within 1180 nT. It can be concluded that the pipeline length will not affect the detection result. In Figure 11(a), since the length of the line is constant, when the pipe length becomes shorter, magnetic leakage will occur at both ends of the pipe. There will be slight changes at both ends of the measuring line as the pipe length decreases.

3.2.3. Permeability. Permeability is the physical nature of the iron pipeline which differentiates it from the surrounding soil and fluid in the pipe. The permeability of the pipeline is usually several orders of magnitude higher than that of the surrounding medium [14, 25]. In the reference model, the permeability of the pipeline is specified to be from 100 and 900 with an interval of 200. The influence of permeability of the pipeline on MF is presented in Figure 12.

The simulation results show that the permeability of the pipeline will have a significant effect on the MF. With the increase in permeability, the magnetic anomaly fluctuates less which decreases from 2400 nT to 1200 nT. The reason is that when permeability increases, the magnetic field of the permanent magnet will be shielded more and the MF on the measuring line will be reduced accordingly.

3.2.4. Permanent Magnets. The magnets are the magnetic source for MAD and therefore are of vital importance [20, 21]. The magnets mounted on the pig can be set up with different numbers with different arrangements. In order to study the effect of different numbers of permanent magnets on detection of MF, here we assume that the remanence of all the magnets is the same. Figure 13 gives the simulation results when different numbers of magnets are employed.

The simulation results indicate that an increased number of magnets will have no influence on the magnetic anomaly intensity at both ends of the measuring line. But for the magnetic anomaly just above the pig, the effect is quite obvious. With the increase in the number of magnets, the magnitude of MF increases gradually from 300 nT to 1200 nT.

In order to study the influence of the polarity of magnets on the detection of MF, the pig carrying two magnets of the same magnetic moment but different polarity is employed. The two magnets are arranged in two different ways, i.e., horizontal and vertical arrangements, respectively. The simulation results are shown in Figure 14.

From the figure above, it can be seen that the MF is almost 0 when the magnets are deployed in the horizontal way. This is because the magnetic fields generated by the two magnets cancel each other in this way of deployment. When the two magnets are fixed vertically, the MF is about 100 nT. This is because in this case the magnetic field generated by the upper magnet is slightly more than that by the lower magnet and there is a magnetic difference between the two. Compared with the MF caused by other factors, the 100 nT fluctuation by magnetic polarity is relatively small.

3.2.5. Geomagnetic Field. As shown in the geomagnetic coordinate system, the seven geomagnetic elements are the most commonly used for geomagnetic measurement and study [25, 26]. Figure 15 gives the spatial distribution of the geomagnetic field.

In the figure above, F is the intensity of the geomagnetic field, I_c is the magnetic inclination, D is the magnetic declination, and H is the horizontal component of the geomagnetic field. X, Y, and Z are the north, the east, and vertical components, respectively.

The geomagnetic field intensity varies between approximately 22000 nT and 68000 nT [25, 26], with the maximum observed at the two poles and the minimum at the equator. In order to study the influence of geomagnetic intensity on the detection of magnetic anomaly along the measuring line, the geomagnetic intensity is specified to be from 21000 nT to

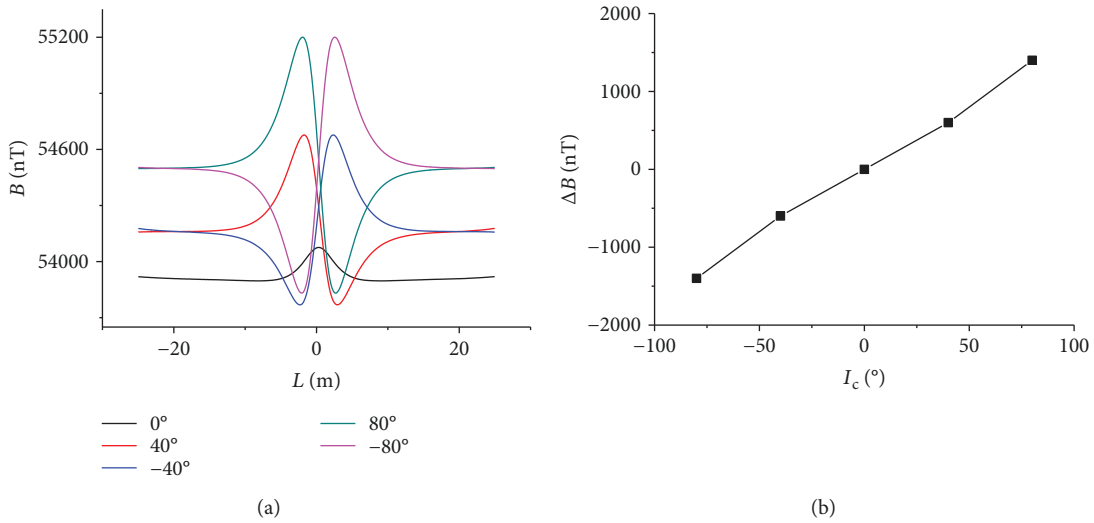

Figure 17: The influence of magnetic inclination on the MF. (a) Five MF curves; (b) the variation trend of MF.

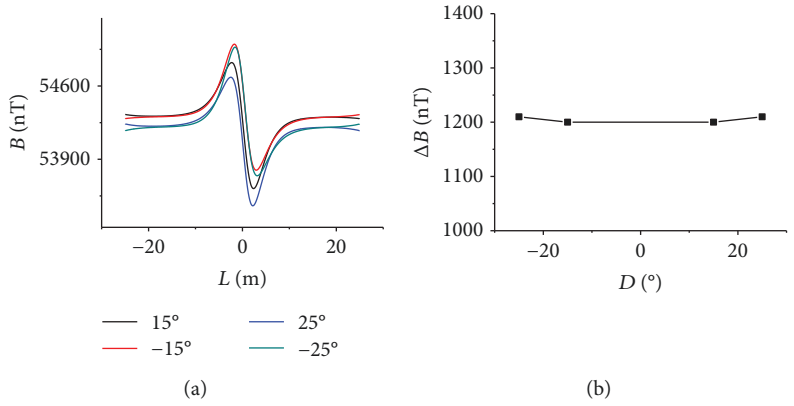

Figure 18: The effect of declination on the MF. (a) Four MF curves; (b) the variation trend of MF.

69000 nT with an interval of 12000 nT in the simulation. Figure 16 gives the simulation results.

As shown in the figure above, with the other model parameters remain unchanged, the increase in geomagnetic intensity will result in a proportional increase in magnetic anomaly. But the MF above the permanent magnets basically remains unchanged.

The geomagnetic inclination reaches 90° at the North Pole, -90° at the South Pole, and 0° at the equator. In order to study the effect of geomagnetic inclination on MF, the inclination is specified to be from -90° to 90° with a certain interval in the simulation. The simulation results are shown in Figure 17.

From the simulation results, it can be seen that with the variation of magnetic inclination from -80° to 80°, the magnetic anomaly measured at the center of the measuring line increases gradually from -1400 nT to 1400 nT. According to Figure 15, the reason is that:

$$F_y = F \times \cos I_c \times \sin D. \quad (4)$$

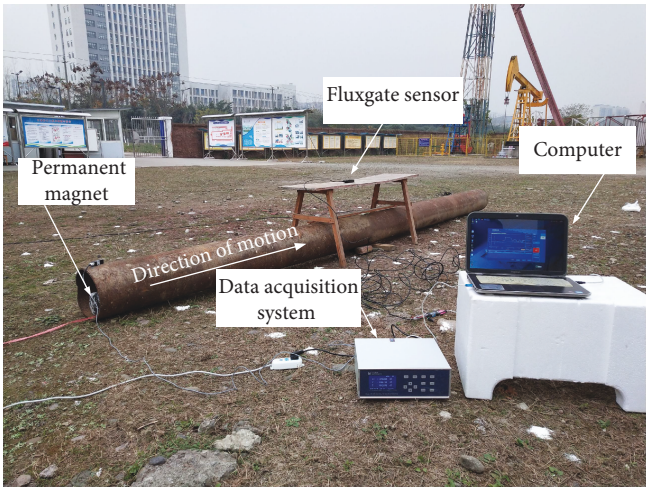

Figure 19: Experimental tool.

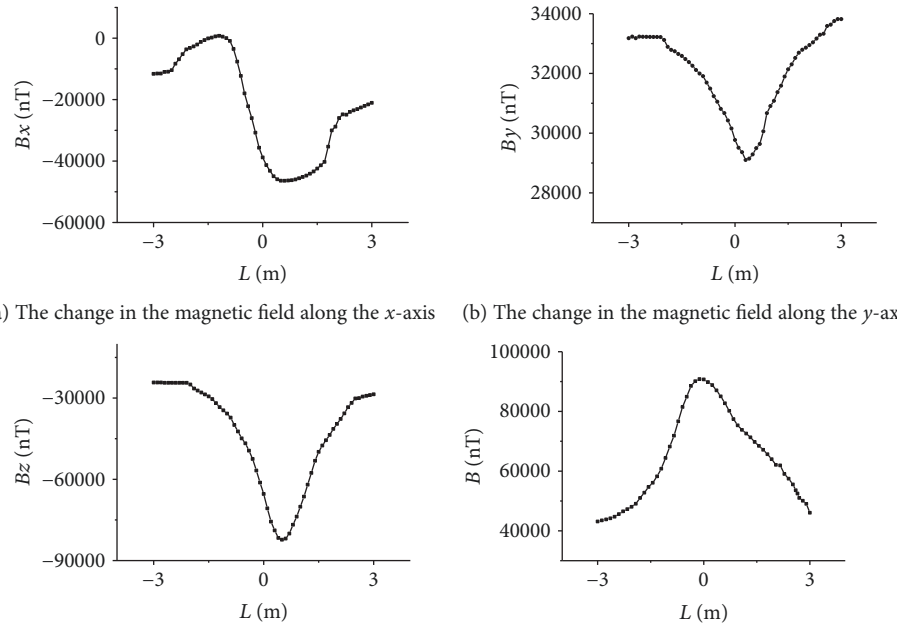

(a) The change in the magnetic field along the x-axis

(b) The change in the magnetic field along the y-axis

(c) The change in the magnetic field along the z-axis

(d) The change in the total field intensity

Figure 20: The experimental results.

With the change of I_c, F_y will increase first and then decrease. This means that the offsetting effect of the geomagnetic field on the magnet field will increase first and then decrease. Consequently, the MF caused by the total magnetic field will decrease first and then increase.

The declination varies from place to place and ranges from -30° to 30°. By specifying the declination to be various values with other model parameters unchanged, the simulation result is obtained as shown in Figure 18.

It can be seen from Figure 18 that with the change of declination, the total magnetic anomaly changes a little. But the MF at the center of the measuring line remains almost unchanged, which is around 1200 nT.

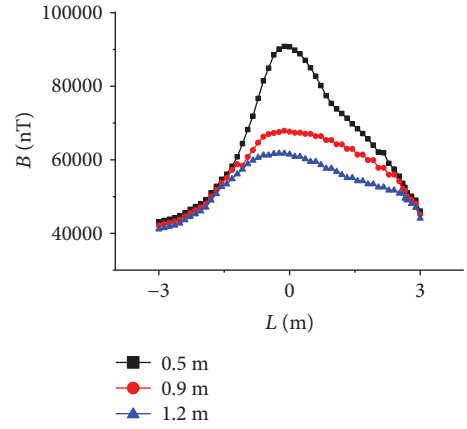

Figure 21: The influence of burial depth on the total field.

4. Experiment

The existing pipe in a laboratory in Chengdu, China, is taken as the research object on the basis of the above numerical simulation to test the magnetic abnormal fluctuation of the measuring point when the pig labeled with magnets passes through the pipe to verify the correctness of the result. Relevant experimental tools on site are shown in Figure 19. The pipe's outer diameter is about 28 cm, the wall thickness is about 4 mm, and the length is about 8 m. The pig is attached with a permanent magnet with a diameter of 50 mm and a length of 60 mm, and the residual magnetism is about 1.2 T, moving from east to west. The fluxgate triaxial sensor is used to detect magnetic anomalies. The 6 m in the middle of the pipe is selected as the measurement range in order to eliminate the influence of magnetic flux leakage at both ends of the pipe and use its supporting data acquisition system and upper computer to display the fluctuation of the magnetic field.

In Figure 19, the sensor is 0.5 m high from the pig, the x-axis of the sensor is parallel to the pipe axis, the y-axis is perpendicular to the pipe axis and points to the right of the picture shown, and the z-axis is perpendicular to the ground as shown above. The magnetic field component value and the total field fluctuation value of the sensor in the direction of x-axis, y-axis, and z-axis are shown in Figure 20.

As shown in Figure 20, there is an obvious fluctuation of the magnetic field value in three directions and the total magnetic field value at the measuring point when the pig passes through. Compared with the numerical simulation results, the fluctuation value of the magnetic field is much higher than the simulated fluctuation value because the pipe is thinner, the wall thickness is thinner, and the measuring point is closer in the experiment. Due to the difference of

Table 1: The influence of each parameter on the magnetic anomaly.

Model parameters	Range	With the increase in the parameter
Pipeline buried depth (mm)	2-3.5	Fluctuation decreases
Existence of permanent magnets	Nonexistent-existent	Obvious fluctuation
Pipeline outer diameter (mm)	500-700	Fluctuation decreases
Pipeline wall thickness (mm)	4-10	Fluctuation decreases
Pipeline length (m)	60-75	Fluctuation almost remains the same
Pipeline permeability	100-900	Fluctuation decreases
Number of permanent magnets	2-6	Fluctuation increases at the center of the measuring line and almost unchanged at both ends
Polarity of permanent magnets	Horizontal-vertical	Fluctuation is negligible
Magnetic intensity (nT)	21000-69000	Fluctuation almost remains the same
Magnetic dip	-80°~80°	Fluctuation decreases first and then increases
Magnetic declination	-25°~25°	Fluctuation almost remains the same
Detection height in the experiment	0.5 m-1.2 m	Fluctuation decreases

geomagnetic parameters, the experimental waveform is different from the simulated waveform. But experimental results show that the principle is correct and the method is feasible by using a magnetic source marker to locate the pig.

Similar to Section 3.2.1, the changes of the total field intensity at the burial depth of 0.9 m and 1.2 m were tested, respectively, to analyze the influence of the buried depth on the magnetic fluctuation value of the measuring point, and the results are shown as Figure 21.

As shown in Figure 21, when the burial depth increases, the fluctuation value of the total field gradually decreases, and the experimental result is consistent with the simulation result. The actual detection results in Figures 20 and 21 confirm the correctness of numerical simulation in this paper to some extent. More experiments are needed to further analyze the accuracy of simulation results. At the same time, it is difficult to study the influence of different geographical locations on the detection results due to geographical restrictions.

5. Results and Discussions

The influence of each model parameter on the magnetic anomaly along the measuring line is summarized in Table 1. As Table 1 shows, the existence of magnets will induce obvious fluctuations to the magnetic field above the magnets which is used to be smooth and stable in absence of the magnets. The fluctuation is subject to various factors. When the number of the magnets is changed, an obvious change in the magnetic field will only occur at the measuring point just above the magnets. The magnetic field at both ends of the measuring line remains almost unchanged. With the increase in buried depth of the pipeline, the MF at the center of the measured line decreases accordingly. With the increase in pipeline outer diameter and wall thickness, the MF decreases. However, with the increase in pipeline length, the MF changes very little. As shown at the end of Table 1, for the experimental results, when the detection height is changed, the magnetic field fluctuation on the measurement line gradually decreases, which is consistent with the simulation results.

6. Conclusions

In this paper, a mathematical model for detection of MF induced by the magnet-labelled pig is proposed. Instead of analyzing the MF at a measuring point, a measuring line is employed for detection and analysis. Furthermore, the influences of pipeline geometries, magnet configuration, and geomagnetic characteristics on the distribution of magnetic anomalies are analyzed in detail. The study results show that the existence of magnets will have an obvious effect on the magnetic distribution, and therefore, it is feasible to detect the magnet-labelled pig by analyzing the MF induced. The magnetic anomaly distribution along the measuring line is subject to various factors such as the buried depth of the pipeline, the pipeline geometries, the geomagnetic field, the permeability of the pipeline, and the number of permanent magnets. When the pig passes the measuring point, an obvious MF will be observed. By comparing the MF curve of the measuring point with magnetic anomaly of the measuring line, it can be seen that the two undergo the same trend and the central MF of the two methods is the same. With the increase of magnets, the magnetic anomaly at both ends of the measuring line almost remains unchanged, while the magnetic anomaly just above the magnets will experience an obviously enhanced fluctuation. Based on this, magnetic detection can be more easily achieved by increasing the number of magnets. But attention should be paid to the direction of magnets during installation so as to make sure that the magnetic fields thereof will not offset each other. The numerical simulation in this paper reveals the interrelation between each model parameter and the measured result. In general, the feasibility of monitoring pig movement by employing magnet-labelled pigs is well proved. At last, the experiment was carried out in a laboratory in Chengdu, China, and the experimental results verify the correctness of the simulation to some extent. At the same time, further experimental comparison and analysis will be the next research direction.

Data Availability

(1) The [Geometric model] data used to support the findings of this study are included within the article. (2) The [Influence of parameters] data used to support the findings of this study are included within the article. (3) The [Figures] data used to support the findings of this study are included within the article.

Conflicts of Interest

The authors declare that there is no conflict of interest regarding the publication of this paper.

Acknowledgments

This work is supported by the National Natural Science Foundation of China under Grant No. 41374151, the Sichuan Province Applied Basic Research Project (No. 2017JY0162), and the Young Scholars Development Fund of SWPU (No. 201599010079).

References

[1] Z. Liang, H. He, and W. Cai, "Speed simulation of bypass hole PIG with a brake unit in liquid pipe," *Journal of Natural Gas Science and Engineering*, vol. 42, pp. 40–47, 2017.

[2] H. Zhang, S. Zhang, S. Liu, Y. Wang, and L. Lin, "Measurement and analysis of friction and dynamic characteristics of PIG's sealing disc passing through girth weld in oil and gas pipeline," *Measurement*, vol. 64, pp. 112–122, 2015.

[3] H. Qiu, H. Wang, W. Sun, X. Zhao, B. Li, and C. Chen, "Present and future development of pig tracing and positioning techniques," *Oil & Gas Storage and Transportation*, vol. 34, no. 10, pp. 1033–1037, 2015.

[4] I. C. P. Blanco, J. H. P. Alvarez, and G. Dobmann, "Simulation for magnetic flux leakage signal interpretation: a FE-approach to support in-line magnetic pipeline pigging," in *2014 IEEE Far East Forum on Nondestructive Evaluation/Testing*, pp. 20–23, Chengdu, China, June 2014.

[5] X. Gao, S. Yan, and B. Li, "A novel method of localization for moving objects with an alternating magnetic field," *Sensors*, vol. 17, no. 4, p. 923, 2017.

[6] W. Zhao, X. Huang, S. Chen, Z. Zeng, and S. Jin, "A detection system for pipeline direction based on shielded geomagnetic field," *International Journal of Pressure Vessels and Piping*, vol. 113, pp. 10–14, 2014.

[7] D. Liu, X. Xu, C. Huang et al., "Adaptive cancellation of geomagnetic background noise for magnetic anomaly detection using coherence," *Measurement Science and Technology*, vol. 26, no. 1, article 015008, 2015.

[8] J. E. Mcfee, Y. Das, and R. O. Ellingson, "Locating and identifying compact ferrous objects," *IEEE Transactions on Geoscience and Remote Sensing*, vol. 28, no. 2, pp. 182–193, 1990.

[9] Z. Y. Guo, D. J. Liu, Q. Pan, and Y. Y. Zhang, "Forward modeling of total magnetic anomaly over a pseudo-2D underground ferromagnetic pipeline," *Journal of Applied Geophysics*, vol. 113, pp. 14–30, 2015.

[10] E. Weiss, B. Ginzburg, T. Cohen et al., "High resolution marine magnetic survey of shallow water littoral area," *Sensors*, vol. 7, no. 9, pp. 1697–1712, 2007.

[11] K. Davis, Y. Li, and M. Nabighian, "Automatic detection of UXO magnetic anomalies using extended Euler deconvolution," *Geophysics*, vol. 75, no. 3, pp. G13–G20, 2010.

[12] A. Sheinker and M. B. Moldwin, "Magnetic anomaly detection (MAD) of ferromagnetic pipelines using principal component analysis (PCA)," *Measurement Science and Technology*, vol. 27, no. 4, article 045104, 2016.

[13] S. Feng, D. Liu, X. Cheng, H. Fang, and C. Li, "A new segmentation strategy for processing magnetic anomaly detection data of shallow depth ferromagnetic pipeline," *Journal of Applied Geophysics*, vol. 139, pp. 65–72, 2017.

[14] Y. Zhang, D. Liu, Y. Li, Z. Guo, and Z. Wang, "Numerical simulation of surface high-precision magnetic detection of underground metal pipes," *Journal of China University of Mining & Technology*, vol. 45, no. 1, pp. 183–188, 2016.

[15] P. Furness, "Modelling magnetic fields due to steel drum accumulations," *Geophysical Prospecting*, vol. 55, no. 5, pp. 737–748, 2007.

[16] M. Marchetti, V. Sapia, and A. Settimi, "Magnetic anomalies of steel drums: a review of the literature and research results of the INGV," *Annals of Geophysics*, vol. 56, no. 1, pp. 1415–1422, 2013.

[17] J. McFee and Y. Das, "Determination of the parameters of a dipole by measurement of its magnetic field," *IEEE Transactions on Antennas and Propagation*, vol. 29, no. 2, pp. 282–287, 1981.

[18] J. Li, X. L. Zheng, W. S. Hou, J. He, and X. Fang, "Simulation and experimental research of magnetic field produced by permanent magnet used in magnetic localization," *Journal of System Simulation*, vol. 21, no. 18, pp. 5919–5922, 2009.

[19] W. Yang, C. Hu, M. Li, M. Q.-H. Meng, and S. Song, "A new tracking system for three magnetic objectives," *IEEE Transactions on Magnetics*, vol. 46, no. 12, pp. 4023–4029, 2010.

[20] C. Hu, *Localization and Orientation System for Robotic Wireless Capsule Endoscope, [Ph.D. Thesis]*, University of Alberta, Alberta, Canada, 2006.

[21] J. A. Baldoni and B. B. Yellen, "Magnetic tracking system: monitoring heart valve prostheses," *IEEE Transactions on Magnetics*, vol. 43, no. 6, pp. 2430–2432, 2007.

[22] A. Sheinker, L. Frumkis, B. Ginzburg, N. Salomonski, and B. Z. Kaplan, "Magnetic anomaly detection using a three-axis magnetometer," *IEEE Transactions on Magnetics*, vol. 45, no. 1, pp. 160–167, 2009.

[23] U. Marschner and W. J. Fischer, "Indirect measurement of a bar magnet position using a hall sensor array," *IEEE Transactions on Magnetics*, vol. 43, no. 6, pp. 2728–2730, 2007.

[24] S. L. Butler and G. Sinha, "Forward modeling of applied geophysics methods using Comsol and comparison with analytical and laboratory analog models," *Computers & Geosciences*, vol. 42, pp. 168–176, 2012.

[25] C. C. Finlay, S. Maus, C. D. Beggan et al., "International geomagnetic reference field: the eleventh generation," *Geophysical Journal International*, vol. 183, no. 3, pp. 1216–1230, 2010.

[26] "Model field at a point by IGRF," December 2017, http://wdc.kugi.kyoto-u.ac.jp/igrf/point/index.html#MAP.